Practical countermeasures for the aerodynamic performance of long-span cable-stayed bridges with open decks

Rui Zhou[1,2a], Yongxin Yang[*1], Yaojun Ge[1b], Priyan Mendis[2c] and Damith Mohotti[3d]

[1]*State Key Laboratory for Disaster Reduction in Civil Engineering, Tongji University, Shanghai 200092, China*
[2]*Department of Infrastructure Engineering, The University of Melbourne, VIC 3010, Australia*
[3]*School of Civil Engineering, The University of Sydney, NSW, 2006, Australia*

Abstract. Open decks are a widely used deck configuration in long-span cable-stayed bridges; however, incorporating aerodynamic countermeasures are advisable to achieve better aerodynamic performance than a bluff body deck alone. A sectional model of an open deck cable-stayed bridge with a main span of 400 m was selected to conduct a series of wind tunnel tests. The influences of five practical aerodynamic countermeasures on flutter and vortex-induced vibration (VIV) performance were investigated and are presented in this paper. The results show that an aerodynamic shape selection procedure can be used to evaluate the flutter stability of decks with respect to different terrain types and structural parameters. In addition, the VIV performance of Π-shaped girders for driving comfortableness and safety requirements were evaluated. Among these aerodynamic countermeasures, apron boards and wind fairings can improve the aerodynamic performance to some extent, while horizontal guide plates with 5% of the total deck width show a significant influence on the flutter stability and VIV. A wind fairing with an angle of 55° showed the best overall control effect but led to more lock-in regions of VIV. The combination of vertical stabilisers and airflow-depressing boards was found to be superior to other countermeasures and effectively boosted aerodynamic performance; specifically, vertical stabilisers significantly contribute to improving flutter stability and suppressing vertical VIV, while airflow-depressing boards are helpful in reducing torsional VIV.

Keywords: cable-stayed bridge; open deck; aerodynamic shape selection method; aerodynamic countermeasures; flutter stability; vortex-induced vibration performance

1. Introduction

The main girders of long-span open deck bridges are generally made of steel-concrete composites. These bridges can be classified into four types, namely: 1) bridges with a concrete deck slab and steel girders; 2) bridges with a concrete main girder and steel plate; 3) bridges with a multi-layered concrete slab on an orthotropic steel plate; and 4) bridges with top

---

∗Corresponding author, Associate Professor, E-mail: yang_y_x@tongji.edu.cn
[a] Ph.D. Student, E-mail: zhourui_88@163.com
[b] Professor, E-mail: yaojunge@tongji.edu.cn
[c] Professor, E-mail: pamendis@unimelb.edu.au
[d] Ph.D., E-mail: pmdamith2012@gmail.com

and bottom concrete deck slabs and corrugated steel webs. Considering the advantages of the two contrasting properties of steel and concrete, in which steel has strong tensile strength and concrete has great compressive strength, a steel-concrete composite girder can be used effectively as a bridge girder. These composite girders demonstrate many attributes, such as great crossing ability, light weight, low cost, and convenient construction. Also, composite girders can be used to avoid the frequent damage to asphalt concrete pavements, which is prone to happen in steel box girder bridges. Therefore, steel-concrete composite girders have been gradually adopted for many long-span bridges around the world, and have become a very popular design configuration in long-span cable-stayed bridges (Collings 2005). Typical examples include the famous cable-stayed Yangpu Bridge in Shanghai (China) with a main span of 602 m, Qingzhou Min River Bridge in Fuzhou (China) with a main span of 605 m, and the three-tower cable-stayed Erqi Yangtze River Bridge in Wuhan (China) with two main spans of 616 m.

However, the bluff shape and lower torsional rigidity of steel-concrete composite girders generally lead to poor aerodynamic performance when compared with more streamlined steel box girders. Moreover, the structural stiffness declines as the span increases. As a consequence, long-span composite girders are likely to face serious wind-induced vibrations, among which flutter performance plays an important role in structural safety, and vortex-induced vibration (VIV) endangers structural serviceability (Ge and Xiang 2008, Wu and Kareem 2013). In order to mitigate these wind-induced vibrations, practical aerodynamic measures have been successfully applied in many engineering projects, and passive aerodynamic countermeasures have become more attractive from a practical point of view. Overhanging deck and edge plates adopted in the Alex Fraser Bridge (Canada) (Irwin 1984), wind fairings in Long Creek Bridge (Canada) (Wardlaw 1971), airflow-depressing boards in the Dongying Yellow River Bridge (China) with open steel box girders to reduce the amplitude of VIV, and apron boards and guide plates at the edge of the main girder in the Qingzhou Min River Bridge and Nanpu Bridge (China) to increase flutter critical wind velocity (Song *et al*. 2002), can be considered as successful examples of such applications. In addition, an experimental study has been conducted by Murakami *et al.* (2002) to clarify the influence of different central guard fences and rectangular members at the inside of main girders on flutter and VIV performance of the Π-shaped main girder. Furthermore, aerodynamic shape optimisation of a steel-concrete composite cable-stayed bridge with a Π-shaped deck and inclined guide vanes was studied by Dong *et al*. (2012). Many studies on aerodynamic countermeasures are also limited to their effects on either flutter or vortex-induced vibration performance alone, and have not taken into account their comprehensive influence on aeroelastic performance (Larsen and Wall 2012, Laima *et al*. 2013, Yang *et al*. 2015). Moreover, the optimal effectiveness of many practical aerodynamic countermeasures has not been compared in detail, and reasonable aerodynamic shape selection of basic bridge decks has not been provided. In summary, a clear research gap exists for establishing a proper aerodynamic shape optimisation method and selection of countermeasure techniques. An aerodynamic shape selection method for long-span bridges with open decks was first proposed. Wind tunnel experiments were performed on a series of aerodynamic passive countermeasures (including wind fairings, apron boards, horizontal guide plates, vertical stabilisers, and airflow-depressing boards) to suppress wind-induced vibration for a cable-stayed bridge with a 400 m centre span and Π-shaped girder. Based on experimental observations, an aerodynamic shape selection method was proposed, and potential application of different countermeasure techniques was discussed. The effectiveness of aerodynamic countermeasures on both VIV and flutter performance were compared in order to confirm optimisation selection of the control scheme.

2. Aerodynamic shape selection procedure

Overall optimal aerodynamic performance of a bridge deck can be achieved through a reasonable aerodynamic shape selection procedure. The influence of terrain type parameters at the bridge site (determining flutter checking velocity), and structural and shape parameters (determining flutter onset velocity) should be evaluated jointly in flutter performance evaluation. Then, a reasonable aerodynamic shape for the main girder can be determined based on a comprehensive consideration of flutter and stationary aerodynamic instability. Two approaches, including aerodynamic countermeasures and structural parameters adjustment, should be adopted for complex aerodynamic stability problems. Otherwise, VIV performance should be examined at the next stage, as given in Fig. 1. If the selected deck fails to pass VIV performance evaluation, a series of aerodynamic countermeasures should be compared to explore the optimal countermeasure. Afterwards, the verification of flutter, buffeting and VIV performance will be conducted before confirming the final design scheme. The whole aerodynamic shape selection procedure for bridge girders is described in Fig. 1. In this paper, this procedure was mainly adopted to evaluate flutter and VIV performance for the Π-shaped girder bridge and to compare the selection of aerodynamic countermeasures.

3. Experimental model design

A long-span cable-stayed bridge with a composite girder of two steel I-shaped side beams and a concrete deck plate was selected in this study. The bridge has a main span of 400 m, and two inverted 124.5 m high Y-shaped pylons with 48 pairs of cables. The Π-shaped main girder is 29.2 m wide and 3.0 m deep. The structural layouts of the whole bridge and the main girder are shown in Figs. 2(a) and 2(b), respectively.

The wind tunnel experiment on a two-dimensional rigid sectional model of the main girder was conducted in a 3 m (width) × 2.5 m (height) test section of the TJ-2 wind tunnel in Tongji University, China. The geometric scale was 1:60, and the wind speed scales for the flutter and vortex-induced vibration tests were 1:5 and 1:3.5, respectively. The major parameters of the prototype bridge and this sectional model are listed in Table 1.

Table 1 Scaled-down properties of the prototype bridge and sectional model

Properties	Prototype (assumed)	Similarity Ratio	Model (scaled)
Width (B)	29.2 m	1:60	0.487 m
Depth (D)	3.0 m	1:60	0.05 m
Mass (M)	38 801 kg/m	$1:60^2$	10.78 kg/m
Inertia (I)	2 864 466 kg·m^2/m	$1:60^4$	0.221 kg·m^2/m
Damping (ζ)	0.01	1:1	0.01
Vertical frequency (f_v)	0.358 Hz	17.4:1	6.229 Hz
Torsional frequency (f_t)	0.722 Hz	17.4:1	12.588 Hz

Fig. 1 Aerodynamic shape selection procedure for bridge girders
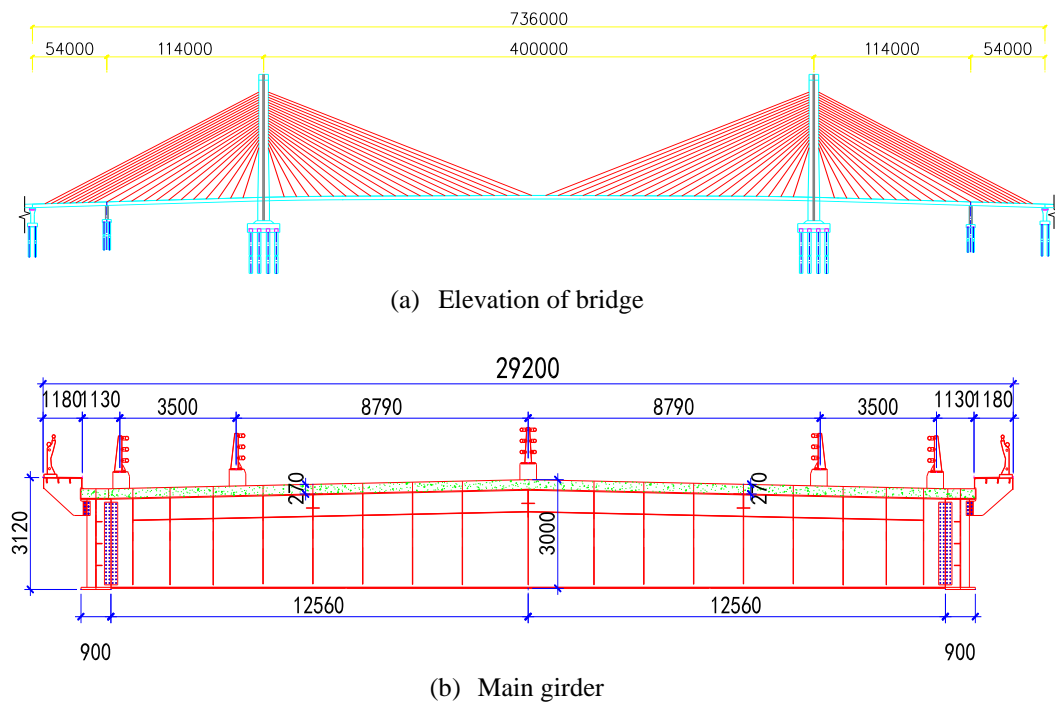

(a) Elevation of bridge

(b) Main girder
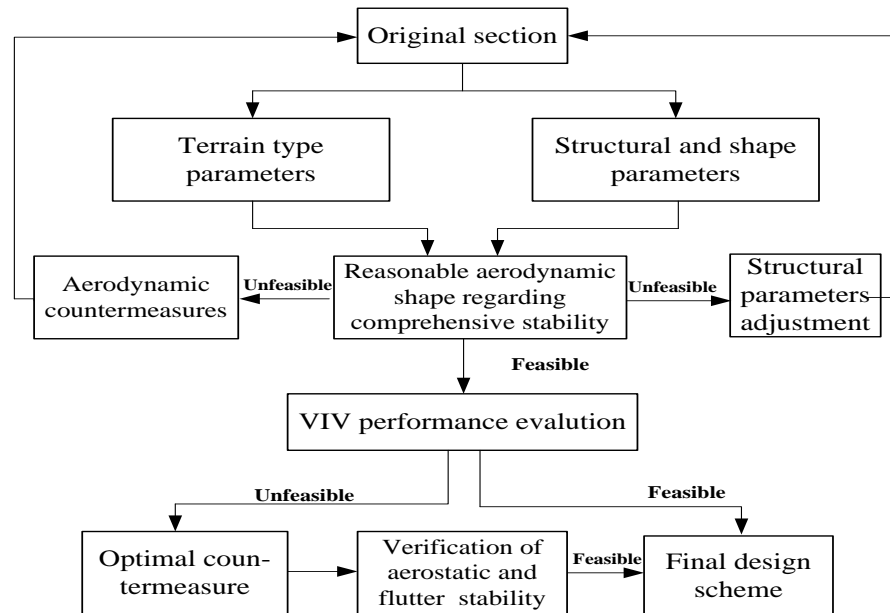
Fig. 2 Structural layout of a cable-stayed bridge (unit, mm)

4. Results and discussion

4.1 Flutter stability evaluation of Π-shaped girder

When the ratio of torsional and vertical frequency exceeds 1.5, the torsional frequency of a cable-stayed bridge will play a leading role in determining the flutter critical wind velocity. The torsional frequency of a bridge with a Π-shaped girder is much higher than that of a bridge with a closed steel box girder due to the relative lower free torsional stiffness. It is noted that a high torsional-vertical frequency ratio of a cable-stayed bridge with an open deck effectively improves the flutter performance and positively contributes to the flutter stability.

The flutter test of the original section was conducted in smooth flow, and flutter derivatives were identified by the improved least squares method (Scanlan and Tomko 1971). Three wind attack angles (+3°, 0° and -3°) were selected in all these tests. The relationships of the total damping ratios (including the mechanical damping and aerodynamic damping) and the reduced wind speed under the three wind attack angles are presented in Fig. 3. The results showed that the minimum value of the flutter onset velocity was $[U_{cr}'] = 60$ m/s for the wind attack angle of +3°.

4.1.1 Influence of terrain type parameters at the bridge site

According to the Chinese specification JTG/T D60-01-2004, 'Wind-resistant design specification for highway bridges' (given by the Chinese Ministry of Communications), the flutter checking velocity $[U_{cr}]$ of a long-span cable-supported bridge can be defined as follows

$$[U_{cr}] = 1.2\mu_f U_d = 1.2\mu_f\ U_{10}(\frac{z}{10})^\alpha \tag{1}$$

where μ_f is the modification coefficient considering the wind fluctuation and surface roughness, which are related to terrain type at the bridge site; U_{10} is the basic wind velocity at the reference height of 10 m; z is the maximum height of the main girder above ground surface or water surface; and α is the surface roughness coefficient, which is related to the terrain type at the bridge site.
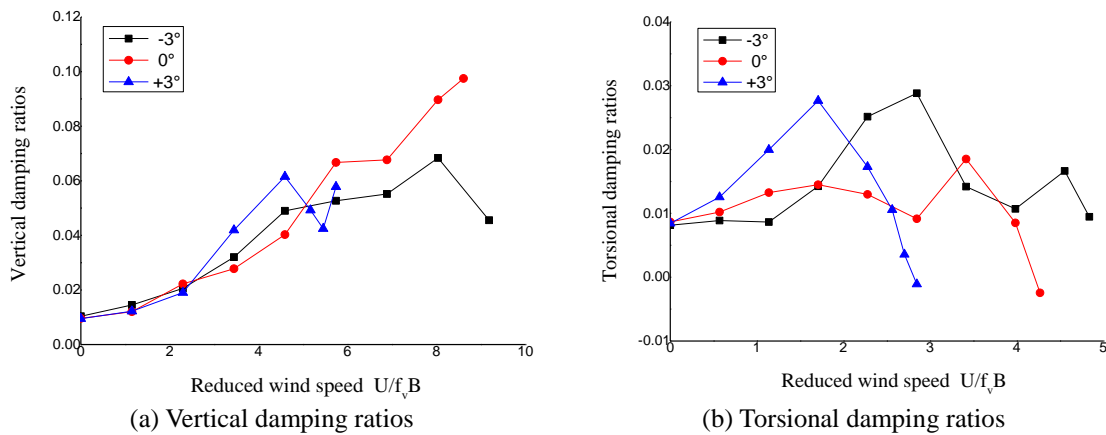

(a) Vertical damping ratios   (b) Torsional damping ratios

Fig. 3 Damping ratios of the original section with reduced wind speed

The maximum allowable wind velocity, $[U_{10}]_{max}$, at the bridge site can be calculated using Eq. (2), if the flutter checking velocity $[U_{cr}]$ is equalled to the onset value of $[U_{cr}'] = 60$ m/s, where $z = 26.86$ m, $\mu_f = 1.29$ and $\alpha = 0.16$, since the bridge site belongs to the B terrain type (JTG/T D60-01-2004).

$$[U_{10}]_{max} = U_d/((\tfrac{z}{10})^{\alpha}) = [U_{cr}]/(1.2\mu_f(\tfrac{z}{10})^{\alpha}) = 60/(1.2 \times 1.29 \times \left(\tfrac{26.86}{10}\right)^{0.16}) = 33.1 \text{ m/s} \quad (2)$$

The allowable wind velocity of $[U_{10}]_{max} = 33.1$ m/s is much higher than the U_{10} value of 23.9 m/s for this cable-stayed bridge, which indicates that the flutter stability of the original section obviously can meet the specification requirement. This implies that similar types of cable-stayed bridges cannot be established in some parts of China, including some coastal cities, which show high U_{10} values (higher than 33.8 m/s in Shanghai).

For further consideration, the influence of terrain type on the bridge site should be discussed. Four terrain types are defined in the Chinese specifications according to the distribution of architecture and geographic position. The calculated values of the maximum allowable wind velocity $[U_{10}]_{max}$ (corresponding to $[U_{cr}'] = 60$ m/s) and the flutter checking velocity $[U_{cr}]$ (corresponding to $U_{10} = 33.8$ m/s in Shanghai) for these four terrain types are listed in Table 2.

According to Table 2, if the terrain type at a bridge site is assumed to be the same as the cable-stayed Yangpu Bridge in Shanghai (with $U_{10} = 33.8$ m/s), only the $[U_{10}]_{max}$ of terrain type A gives values higher than $U_{10} = 33.8$ m/s. However, the $[U_{cr}]$ of terrain type A is smaller than the $[U_{cr}']$ of 60 m/s, which indicates that only terrain type A of Shanghai could be used to establish this bridge at the original bridge site. The high building density regions with B, C and D terrain types in Shanghai could not meet the flutter requirement for similar bridge types. Therefore, the terrain type selection for a bridge site could be estimated by the maximum allowable wind velocity, or the flutter checking velocity.

4.1.2 Influence of structural parameters

The first structural torsional frequency and the shape factor for a main girder of a cable-stayed bridge are directly proportional to the flutter onset velocity according to the following simplified practical formula shown in Eq.(3) (JTG/T D60-01-2004)

$$[U_{cr}'] = \eta_s \cdot \eta_\alpha \cdot U_{cr0} = \eta_s \cdot \eta_\alpha \cdot \left(2.5 \cdot f_t \cdot B \cdot \sqrt{\mu \cdot \tfrac{r}{b}}\right) = \eta_s \cdot \eta_\alpha \cdot \left(2.5 \cdot \tfrac{c}{\sqrt{L}} \cdot B \cdot \sqrt{\mu \cdot \tfrac{r}{b}}\right) \quad (3)$$

where η_s and η_α are modification factors for the shape of the main girder section with regard to the structure and wind attack angle, respectively; f_t represents the basic torsional frequency; L and B are the main span length and the width of the main girder, respectively; and C is a constant reflecting the influence of girder section type.

If the flutter onset velocity $[U_{cr}']$ is assumed as the limit value of 41.7 m/s at the bridge site (defined in the Chinese specification JTG/T D60-01-2004), the maximum possible span length is increased to $[L'] = 2.07L = 828$ m without the influence of other factors, as shown in Eq.(4). In other words, the length of the main span with a Π-shaped girder can be increased to 828 m from the perspective of flutter stability of bridges with two towers at this location.

$$[L'] = (\tfrac{C \cdot B \cdot \sqrt{\mu \cdot \tfrac{r}{b}} \cdot \eta_s \cdot \eta_{\alpha'}}{U_{cr}})^2 = L(\tfrac{U_{cr'}}{U_{cr'}})^2 = 400 \times (\tfrac{60}{41.7})^2 = 828 \text{ m} \quad (4)$$

Table 2 $[U_{10}]_{max}$ and $[U_{cr}]$ of the four terrain types

Type	Surface status	α	μ_f	$[U_{10}]_{max}$ (m/s)	$[U_{cr}]$ (m/s)
A	sea, coast, desert	0.12	1.24	35.8	56.6
B	field, countryside, jungle	0.16	1.29	33.1	61.3
C	hill country, low-rise building concentration areas	0.22	1.35	32.4	68.1
D	high-level building concentration areas	0.30	1.40	30.0	76.4

Table 3 $[L']$ for the four terrain types

Type	Surface status	α	$[U_{cr}']$ (m/s)	$[L']$ (m)
A	sea, coast, desert	0.12	40.0	900
B	field, countryside, jungle	0.16	41.7	828
C	hill country, low-rise building concentration areas	0.22	44.2	737
D	high-level building concentration areas	0.30	47.8	630

The maximum allowable main span length $[L']$ for the four terrain types are calculated and listed in Table 3, and the $[L']$ for terrain types A and D are 900 m and 630 m, respectively. Based on a decent flutter performance of the cable-stayed bridge with a Π-shaped girder, this type of main girder could be adopted in cable-stayed bridges with even longer main spans.

4.2 VIV performance evaluation of Π-shaped girder

Compared with cable-stayed bridges with closed steel box girders, the Π-shaped girder cable-stayed bridges with main spans of 200 to 600 m have a higher structural natural frequency. This is closer to the frequency of vortex shedding, which easily leads to a VIV phenomenon based on the knowledge of existing bridges. Due to the potential VIV of cable-stayed bridges with open decks, it is necessary to accurately evaluate their VIV performance by wind tunnel tests.

The VIV responses of the original section with a Π-shaped girder in smooth flow under three wind attack angles of -3°, 0° and +3° are compared in Fig. 4.

As shown in Fig. 4, the most unfavourable behaviour is given by the wind attack angle of +3°. The maximum normalised amplitude of the vertical (relative to the depth of the main girder) and torsional responses are 0.117 and 0.415, respectively. The reduced lock-in wind speed regions of the vertical and torsional VIV are very large, ranging from 1.44 to 2.41 for vertical vibration, and from 1.08 to 1.49 for torsional vibration.

According to the Japanese specification 'Wind-resistant design specification for road bridges' (Japan Road Association, 1991) and driving comfortableness evaluation based on Sperling

evaluation standards (Garg and Dukkipati 1984), the vertical weighting coefficient $F(f)$ is related to the vibration frequency f, as given below

$$F(f) = 0.325f^2 = 0.325 * 0.358^2 = 0.042 \tag{5}$$

Similarly, the driving comfortableness index, W, can be calculated as follows

$$W = 2.7\sqrt[10]{z_0^3 f^5 F(f)} = 2.7\sqrt[10]{0.355^3 \times 0.358^5 \times 0.042} = 0.860 < 1 \tag{6}$$

(where $z_0 = 0.117 \times 3.00.355$).

Although the feel of vibration for passengers based on Sperling evaluation standards is only a slight vibration and completely meets with the driving comfortableness specification, the maximum normalised amplitude of the vertical response in smooth flow is $0.117 > 10\%$, so the amplitude of vertical VIV should not be neglected.

According to structural safety evaluation based on the Chinese specification (JTG/T D60-01-2004), the amplitude limit of VIV responses in the vertical and torsional direction in smooth flow are $[h_b] = 0.04/f_b = 0.04/0.358 = 0.111$ m, $[\theta_\alpha] = 4.56/Bf_t = 4.56/(29.2 \times 0.722) = 0.216°$, where f_b and f_t represent the bending and torsional frequency of the prototype bridge, respectively; and B is the width of the main girder. As shown in Fig. 4, the maximum normalised amplitude of the vertical and torsional responses are 0.117 and 0.415, which are much larger than the normalised amplitude limit of 0.037 (which is equal to $[h_b]/$ depth of the main girder) and 0.216, respectively. Therefore, aerodynamic countermeasures should be adopted to mitigate VIV responses in order to comprehensively consider driving comfortableness and structural safety evaluation.

5. Aerodynamic VIV control measures

Since the peak of VIV responses at smooth flow are much larger than the verification limit values, it is necessary to adopt effective passive aerodynamic countermeasures to mitigate the VIV responses.

(a) Vertical response   (b) Torsional response
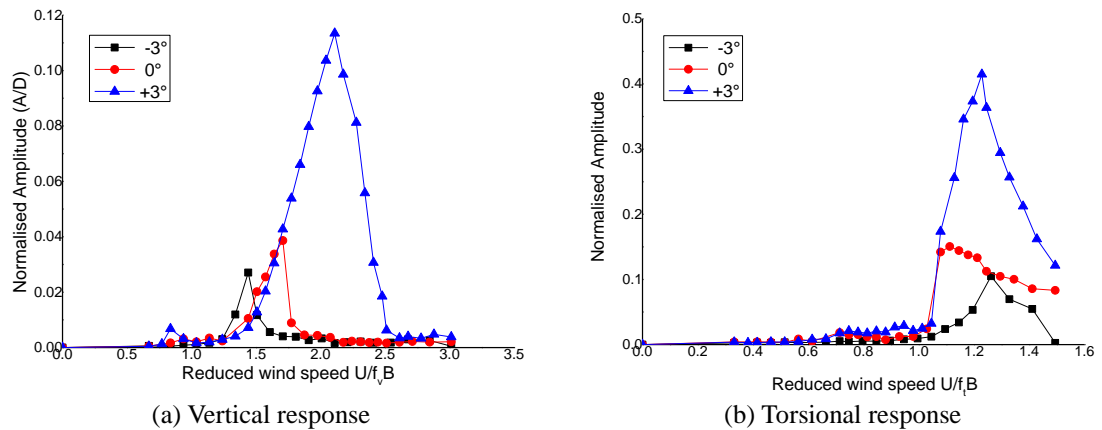
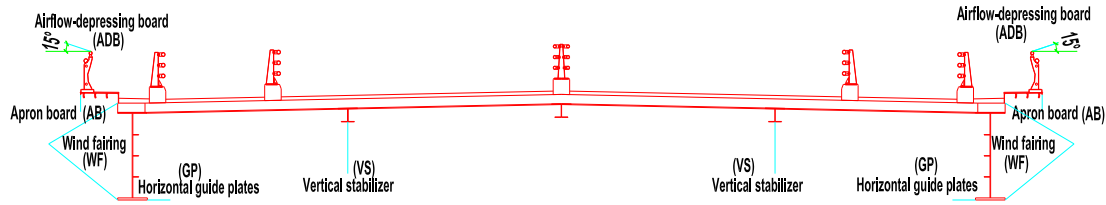Fig. 4 Response comparison of VIV in smooth incoming flow

Fig. 5 Schematic diagram of the five countermeasures

Five common aerodynamic countermeasures were considered in the current investigation: 1) apron boards with a height of 0.5 m (16% of the total deck width); 2) wind fairings with three angles of 45°, 50° and 55°; 3) horizontal guide plates with three lengths of 0.84 m (3% of the total deck width), 1.44 m (5% of the total deck width) and 2.04 m (7% of the total deck width); 4) vertical stabilisers with a height of 1.5 m, which is 50% of the depth of the Π-shaped steel girder; and 5) airflow-depressing boards with a length of 0.84 m (3% of the total deck width) and an inclined angle of 15°. The schematic diagram of these five countermeasures is shown in Fig. 5.

5.1 Apron boards

Based on the flow motion trial of computational fluid dynamics (CFD) calculation results (Sarwar and Ishihara 2010), we find that the mainstream airflow is navigated to the wake airflow by the backflow zone between the leeward girders and the apron boards. Furthermore, the apron boards (AB) are helpful in improving the flutter stability since they guide the mainstream airflow to pass the lower edge of the windward girder more smoothly, and reduce the intensity of vortex separation. The VIV control effect of the apron boards on Π-shaped girders, and a comparison of normalised VIV responses for the open deck with and without apron boards was conducted and is presented in Fig. 6.
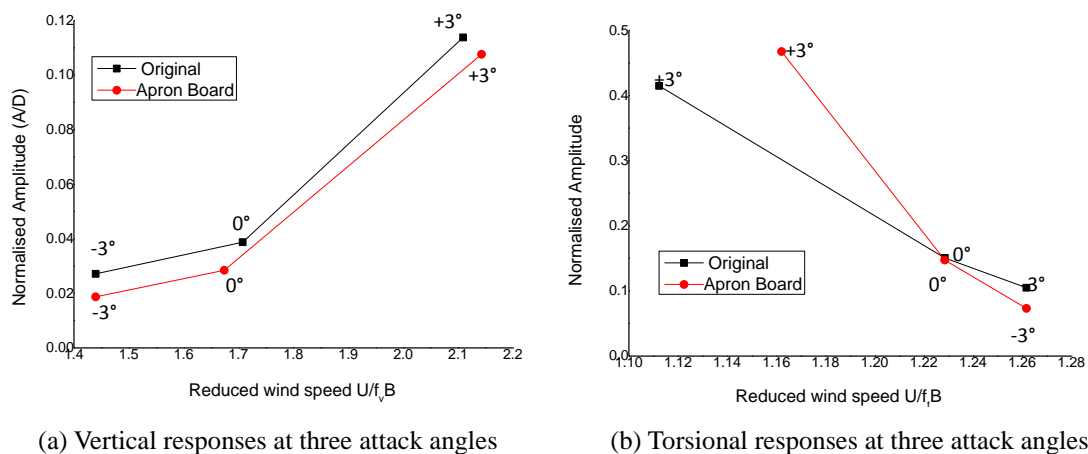

(a) Vertical responses at three attack angles (b) Torsional responses at three attack angles

Fig. 6 Response comparison of VIV with/without apron boards

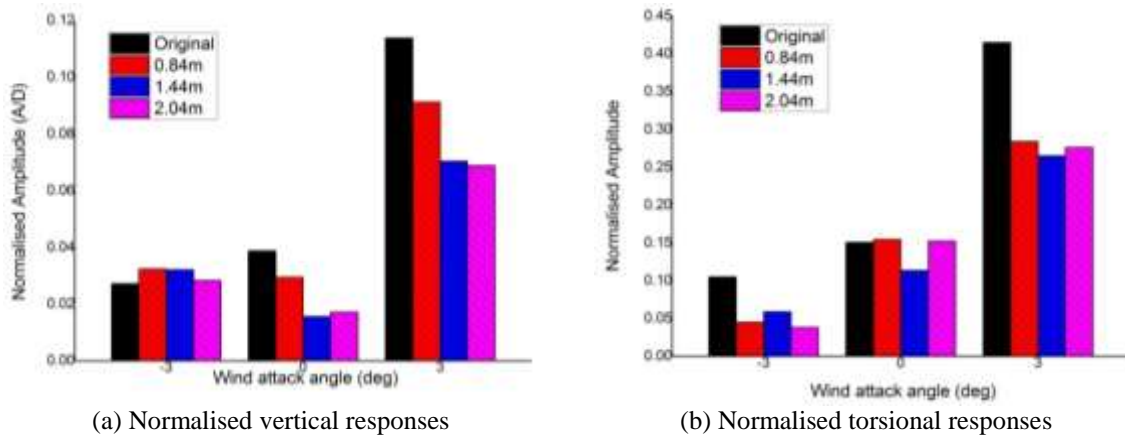(a) Normalised vertical responses (b) Normalised torsional responses

Fig. 7 Response comparison of VIV with/without guide plates

All the maximum values of the vertical responses under the three wind attack angles with apron boards are slightly less than those without apron boards. The maximum value of the torsional response at +3° wind attack angle with apron boards is inferior to the original section, as seen in Fig. 6. As a result, the apron boards can decrease the VIV responses of the open deck to some extent, but this is not an effective method.

5.2 Horizontal guide plates

As a widely used aerodynamic countermeasure in long-span bridges, the guide plates have a significant control effect on VIV (for example, on the Great Belt East Bridge in Denmark). The basic principle is that the airflow in the tail region of the main girder is navigated far away from the mainstream wake district after installing the guide plates. This suppresses the generation of vortex, or the vortex is navigated far away from the main girder region by the guide plate to inhibit the VIV formation (Song *et al.* 2002). The VIV responses of the three widths of the horizontal guide plates at the bottom of the inside of the main girder were compared in Fig. 7, in which the reduced wind velocities at the maximum response points are shown at the top of these charts..

It is very interesting that the horizontal guide plates have a great control effect on mitigating the vertical and torsional vibration for any width of guide plates under the three given wind attack angles. Both the 1.44 m (5% of the total deck width) and 2.04 m (7% of the total deck width) widths of guide plates perform better than the smallest width plate of 0.84 m, especially for vertical vibration under the most unfavourable attack angle of +3°. For the guide plates of 1.44 m width under a wind attack angle of +3°, the maximum normalised vertical and torsional responses are decreased from 0.115 to 0.071, and from 0.41 to 0.27, respectively. Although the guide plates are effective for reducing the VIV amplitude, all these maximum responses of VIV with guide plates were still larger than the corresponding amplitude limit values. As a consequence, other available measures should be explored to thoroughly solve the VIV problem.

5.3 Wind fairings

In general, wind fairings at the edges of a cross-section can smooth the airflow around the main girder and suppress vortex shedding to effectively improve the aerodynamic performance of a bluff body (Wardlaw 1971). VIV responses of an open deck with three angles of wind fairings are presented in Table 4 in order to determine the optimal angle. It is noted that the control effect of a case is defined as follows: Control effect = (Maximum amplitude of the case – Maximum amplitude of the corresponding original section without wind fairings) / (Maximum amplitude of the corresponding original section without wind fairings).

Table 4 shows that wind fairings are effective in reducing VIV amplitudes under the wind attack angle of +3° for all configurations by approximately 50% in vertical responses and 36% in torsional responses. The results for the two remaining wind attack angles show opposite results to the other. More lock-in wind speed regions appeared in vertical vibration, especially under the wind attack angle of 0° at higher wind speed regions.

Table 4 Characteristic parameters of vortex-induced vibration of sections with wind fairings

Angles	Vibration	Attack angle	Lock-in region	Max. normalised amplitude	Reduced wind velocity at peak	Control effect
45°	Vertical	+3°	1.47–1.82	0.058	1.72	48.7%
		0°	2.48–2.68	0.038	2.58	0.74%
		-3°	1.51–2.05	0.064	1.94	-136.1%
50°	Vertical	+3°	1.47–1.81	0.054	1.70	52.7%
		0°	2.14–2.72	0.046	2.44	-19.1%
		-3°	1.38–2.01	0.059	1.90	-118.42%
55°	Vertical	+3°	1.47–1.81	0.051	1.70	54.9%
		0°	2.05–2.81	0.069	2.65	-77.0%
		-3°	1.34–2.01	0.063	1.86	-131.4%
Angles	Vibration	Attack angle	Lock-in region	Max. normalised amplitude	Reduced wind velocity at peak	Control effect
45°	Torsional	+3°	1.00–1.49	0.238	1.20	42.6%
		0°	0.86–1.49	0.451	1.17	-199.5%
		-3°	1.00–1.49	0.193	1.22	-84.0%
50°	Torsional	+3°	1.00–1.33	0.265	1.13	36.1%
		0°	0.88–1.53	0.511	1.20	-239.3%
		-3°	0.98–1.58	0.249	1.25	-137.4%
55°	Torsional	+3°	1.00–1.33	0.296	1.13	28.6%
		0°	0.90–1.49	0.440	1.19	-192.2%
		-3°	0.96–1.49	0.213	1.18	-103.1%

These maximum responses of VIV with a 55° angle fairing are relatively less than those of 45° and 50° for torsional VIV, which indicates that 55° is the best among the three above angles for mitigation of VIV responses. Obviously, wind fairing is not an excellent choice of aerodynamic countermeasure to improve VIV performance of Π-shaped girders.

5.4 Vertical stabilisers

Vertical stabilisers (VS) are also possible aerodynamic countermeasures since the stabilisers play an important role in airflow separation, which have been validated in many practical projects for improving aerodynamic performance, such as the Annacis Severn Bridge (Canada) and Runyang Yangtze River Highway Bridge (China).

5.5 Airflow-depressing boards

For the open deck with a separated rectangular steel box of Dongying Yellow River Bridge (China), the airflow-depressing boards (ADB) with a width of 1.2 times the height of the railing posts and an inclined angle of 10°, had effectively decreased half of the amplitude of VIV responses, which indicates that ADB have the function of disrupting airflow motion and destroying vortex formation (Dong *et al*. 2012).

5.6 Combination of VS and ADB

Three test conditions, including a section with vertical stabilisers alone (VS), airflow-depressing boards (ADB) alone, and a combination of airflow-depressing boards and vertical stabilisers (VS+ADB), were carried out. The VIV responses obtained for the most unfavourable case of +3° wind attack angle are presented in Fig. 8.

The results from Fig. 8(a) show that the control effect of vertical stabilisers in vertical VIV is superior to that of airflow-depressing boards, which is opposite to the control effects in torsional vibration in Fig. 8(b). This is because the maximum normalised amplitudes of the torsional response with only vertical stabilisers is larger than that without vertical stabilisers (original deck). In other words, vertical stabilisers are good at suppressing the vertical vibration, and airflow-depressing boards have a remarkable effect on mitigating the torsional vibration. Hence, the combination of vertical stabilisers and airflow-depressing boards (VS+ADB) are explored to solve the VIV problem of the Π-shaped girder. Figs. 8(a) and 8(b) also demonstrate that the maximum normalised amplitudes of the vertical and torsional response of the original section with a combination of countermeasures at +3° wind attack angle are: 0.03 at the reduced wind speed of 1.74, and 0.12 at the reduced wind speed of 1.13, respectively; all of which are below the corresponding amplitude limit values. Both vertical and torsional responses at the two other wind attack angles are still less than those of the +3° attack angles in Figs. 8(c) and 8(d). Therefore, the combination of vertical stabilisers and airflow-depressing boards are a perfect VIV countermeasure for Π-shaped girders.

5.7 Comparison of different aerodynamic measures

The VIV control effects of the main girder with all these countermeasures for both the vertical and torsional direction under +3° wind attack angle are listed in Table 5, where the maximum

relative amplitudes of vertical response is equal to the maximum vertical response/height of the main girder.

6. Effectiveness on flutter performance

Due to the diverse mechanism of flutter and vortex-induced vibration, passive aerodynamic countermeasures generally have different control effects on these two types of wind-induced vibrations. The flutter performance of sections with horizontal guide plates of three different widths, wind fairings of three different angles, and four mixed measures of vertical stabilisers and air-depressing boards were evaluated using wind tunnel tests in smooth flow. The flutter onset velocities of the above cases and their growth rates are compared in Fig. 9.

Focussing on the flutter control effects of these aerodynamic countermeasures in Figs. 9(a)-9(c), the flutter onset velocities under +3° wind attack angle are the lowest among the three angles considered.

(a) Vertical responses at attack +3°   (b) Torsional responses at attack +3°

(c) Vertical responses under VS+ADB   (d) Torsional responses under VS+ADB

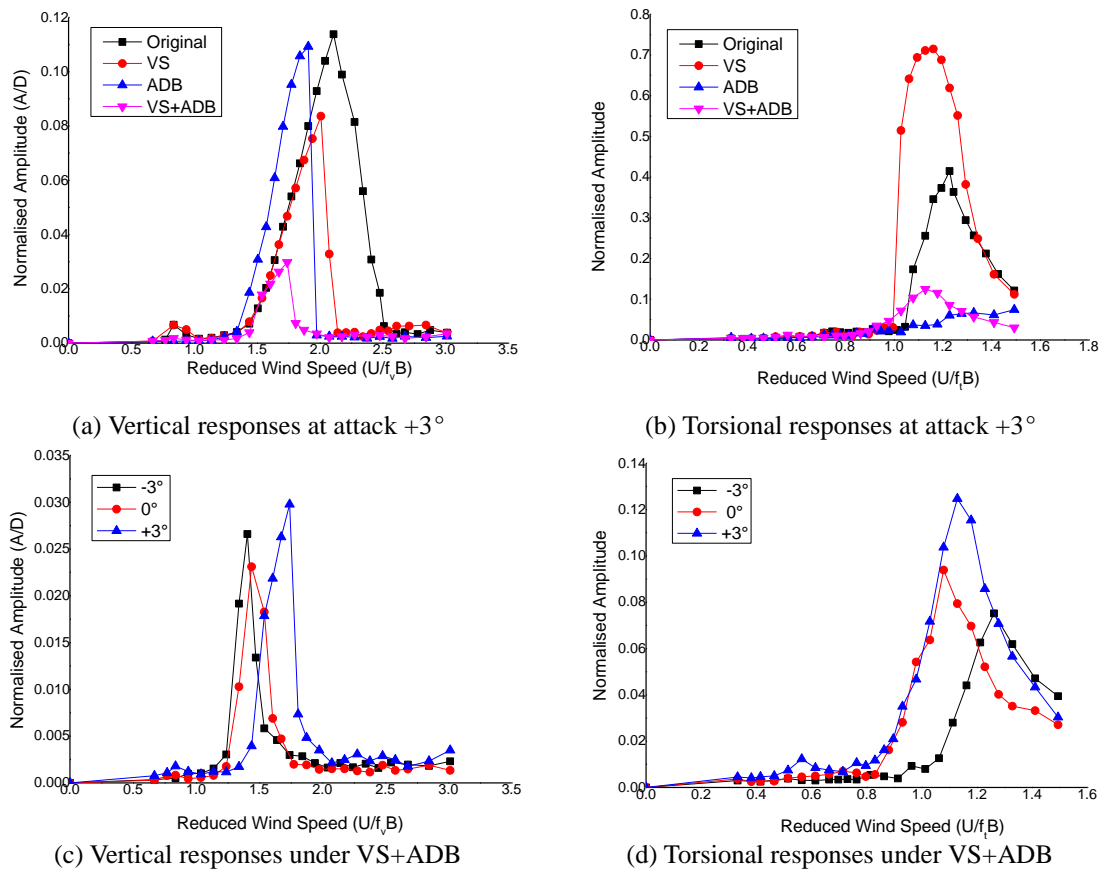Fig. 8 Response comparison of the VIV with vertical stabilisers and airflow-depressing boards

Table 5 Control effects of countermeasures at +3° wind attack angle

Measures	Vibration	Parameters	Lock-in region	Max. normalised amplitude	Control effect
Original	Vertical		1.71–2.34	0.038	
Apron boards	Vertical	0.5 m	1.67–2.54	0.036	5.1%
Guide plates	Vertical	0.84 m	1.68–2.28	0.030	19.5%
		1.44 m	1.66–2.18	0.023	38.1%
		2.04 m	1.65–2.15	0.023	39.0%
Wind fairings	Vertical	45°	1.47–1.81	0.020	48.7%
		50°	1.47–1.82	0.018	52.7%
		55°	1.47–1.82	0.017	54.9%
VS	Vertical	VS	1.67–2.01	0.028	26.3%
AB	Vertical	AB	1.58–1.91	0.037	3.9%
Combination	Vertical	VS+AB	1.63–1.65	0.004	88.1%
Measures	**Vibration**	**Parameters**	**Lock-in region**	**Max. normalised Amplitude**	**Control effect**
Original	Torsional		1.08–1.49	0.415	
Apron boards	Torsional	0.5 m	1.06–1.49	0.468	-12.8%
Guide plates	Torsional	0.84 m	1.07–1.43	0.284	31.6%
		1.44 m	1.06–1.36	0.265	36.1%
		2.04 m	1.05–1.35	0.276	33.5%
Wind fairings	Torsional	45°	1.00–1.49	0.238	42.6%
		50°	1.00–1.33	0.265	36.1%
		55°	1.00–1.33	0.296	28.6%
VS	Torsional	VS	1.03–1.49	0.715	-72.3%
AB	Torsional	AB	1.08–1.49	0.074	82.2%
Combination	Torsional	VS+AB	1.06–1.49	0.075	82.0%

This is similar to the VIV amplitude results given in Table 5. Therefore, the attack angle of +3° is the most unfavourable configuration for the wind-resistance performance of Π-shaped girders. The growth rates of the flutter onset speeds for all these control measures compared with the original section are shown in Fig. 9(d). The notations on the x-axes are abbreviations of all the

above cases, and all the flutter onset velocities of the sections with aerodynamic measures are larger than the original sections.

As for the flutter control effect of the horizontal guide plates, it is noteworthy that the 1.44 m wide guide plate (5% of the total deck width) is superior to the 0.84 m wide plate (3% of the total deck width), in which the most obvious change occurred at the +3° wind attack angle. However, the onset velocities of plates with a width of 2.04 m (7% of the total deck width) are not larger than those with a 1.44 m width; and the onset velocities of plates with 1.44 m width are the largest among the three widths at the 0° wind attack angle. It is interesting that the 1.44 m length guide plate is also the best dimension for controlling the VIV amplitude in Fig. 7. Therefore, the guide plate with a second width of 1.44 m is the most reasonable choice for boosting flutter and VIV performance of the Π-shaped girder.

For wind fairings with three different angles, the flutter onset velocity and its growth rate get higher as the angle of fairing increases under all three wind attack angles, as shown in Fig. 9(b), which confirms that the wind fairing can be helpful in improving the flutter performance of this bluff section. It is interesting that the flutter onset velocities with the largest angle of 55° are the highest among the three fairing angles, so 55° is the best wind fairing angle for improving both flutter and VIV performance.
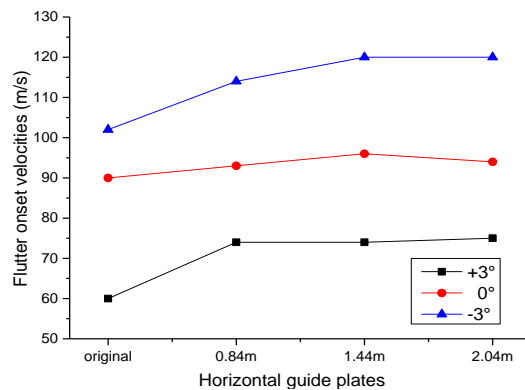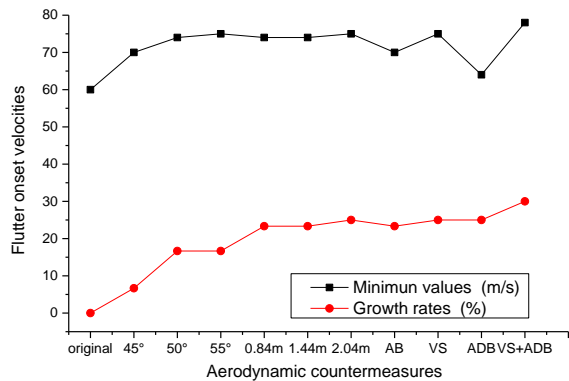

(a) Flutter onset velocities of horizontal guide plates
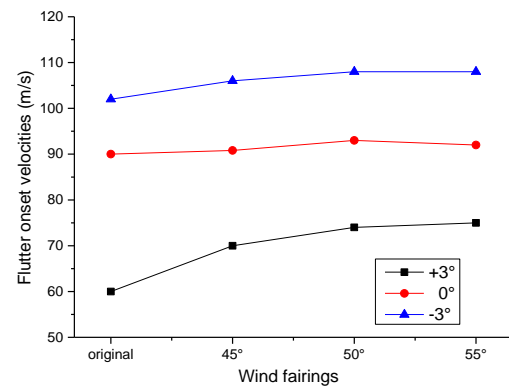
(b) Flutter onset velocities of wind fairings
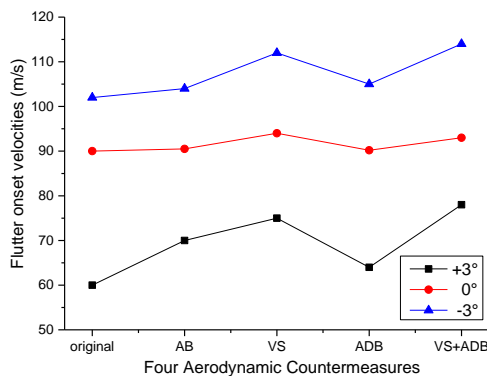
(c) Flutter onset velocities of mixed measures

(d) Flutter onset velocities and their growth rates

Fig. 9 Flutter performance comparison of all aerodynamic countermeasures

Apron boards (AB) can also enhance flutter instability to some extent, especially under the most unfavourable +3° wind attack angle, as shown in Fig. 9(c). However, since it is not effective to mitigate VIV amplitudes, AB are not a preferable aerodynamic countermeasure for Π-shaped girders.

The combination of vertical stabilisers and airflow-depressing boards (VS+ADB) has distinct advantages compared with VS or ADB alone when it comes to the effect of increasing flutter onset velocities; and the growth rates under three wind attack angles of +3°, 0° and -3° are 30.00%, 3.33% and 11.76%, respectively. As shown in Fig. 9(c) and 9(d), the vertical stabiliser (VS) plays a critical role in improving flutter performance, since all the growth rates of flutter onset speeds for vertical stabilisers are much higher than those of airflow-depressing boards (ADB) under the three wind attack angles, which indicates that the vertical stabiliser is an aerodynamic measure to enhance flutter stability for this type of girder section. Considering the VIV control effect of VS, ADB, and VS+ADB, VS not only mitigates the vertical VIV but also enhances flutter performance, while ADB is just helpful in restraining the torsional VIV amplitude. So, VS+ADB is the best solution to improve the aerodynamic performance of this kind of Π-shaped deck.

To sum up, most of these aerodynamic countermeasures are effective in improving flutter and VIV performance, in which the combination of vertical stabiliser and airflow-depressing board is the optimal choice, followed by vertical stabiliser alone, and horizontal guide plate with 5% of the total deck width; and the control effect of an apron board is better than an airflow-depressing board.

7. Conclusions

An aerodynamic shape selection method for long-span bridges with open decks was proposed to guide the selection of five common aerodynamic countermeasures for aerodynamic performance. The conclusions are as follows:

- An aerodynamic shape selection procedure for the main girder of cable-supported bridges is proposed to guide flutter performance evaluation of Π-shaped girders, considering the influence of terrain type structural parameters, and VIV performance evaluation based on driving comfortableness and safety requirements.

- Apron boards are not an effective countermeasure, while guide plates with 5% of the total deck width are a reasonable choice to enhance the flutter stability of this type of open deck among the three different widths, and it is also helpful to improve VIV performance.

- A wind fairing with the largest angle of 55° has the best overall control effect on both VIV and flutter performance of the open deck among the three wind fairing angles, but will lead to more lock-in regions of VIV under 0° wind attack angle.

- The combination of vertical stabilisers and airflow-depressing boards is superior to other countermeasures and has the most positive influence on aerodynamic performance of Π-shaped girders, in which the vertical stabilisers make a great contribution to boost flutter stability and suppress vertical VIV, while airflow-depressing boards help to restrain torsional VIV.

Acknowledgments

References

Collings, D. (2005), *Steel-concrete composite bridges*, Thomas Telford Ltd, London, UK.

Dong, R., Yang, Y.X. and Ge, Y.J. (2012), "Wind tunnel test for aerodynamic selection of Π shaped deck of cable-stayed bridge," *J. Harbin Inst. Tech.*, **44**(10),109-114. (In Chinese)

Garg, V.K. and Dukkipati, R.V. (1984), *Dynamics of railway vehicle systems.* Academic Press, Toronto, Canada.

Ge, Y.J. and Xiang, H.F. (2008), "Recent development of bridge aerodynamics in China", *J. Wind Eng. Ind. Aerod.*, **96**(6-7), 736-768.

Irwin, P.A. (1984), "Wind tunnel tests of long span bridges", *Proceedings of the 12th Congress IABSE*, Vancouver, British Columbia, Canada.

Japanese Road Association (1991), Wind-resistant design specification for road bridges. Maruzen, Tokyo, Japan.

Larsen, A. and Wall, A. (2012), "Shaping of bridge box girders to avoid vortex shedding response", *J. Wind Eng. Ind. Aerod.*, **104-106**,159-165.

Laima, S., Li, H., Chen, W. and Li, F. (2013), "Investigation and control of vortex-induced vibration of twin box girders", *J. Fluids Struct.*, **39**, 205-221.

Ministry of Communication of the People's Republic of China.(2004), JTG/T D60-01-2004 Wind-resistant design specification for highway bridges, China Communications Press, Beijing, China.

Murakami, T., Takeda, K., Takao, M. and Yui, R. (2002), "Investigation on aerodynamic and structural countermeasures for cable-stayed bridge with 2-edge I-shaped girder", *J. Wind Eng. Ind. Aerod.*, **90**(6-7), 2143-2151.

Sarwar, M.W. and Ishihara, T. (2010), "Numerical study on suppression of vortex-induced vibrations of box girder bridge section by aerodynamic countermeasures", *J. Wind Eng. Ind. Aerod.*, **90**(6-7), 2143-2151.

Scanlan, R.H. and Tomko, J.J. (1971), "Airfoil and bridges deck flutter derivatives", *J. Eng. Mech.- ASCE*, **97**(6),1717-1733.

Song, J.Z., Lin, Z.X. and Xu, J.Y. (2002), "Research and Appliance of Aerodynamic Measures about Wind-resistance of Bridges", *J. Tongji Uni (Natural Science Edition)*, **30**(5), 618-621. (In Chinese)

Wardlaw, R.L. (1971), "Some approaches for improving the aerodynamic stability of bridge road decks", *Proceedings of the 3rd Wind Effects on Building and Structures*, Tokyo.

Wu, T. and Kareem, A. (2013), "Vortex-induced vibration of bridge decks: volterra series-based model", *J. Eng. Mech - ASCE*, **139**(12), 1831-1843.

Yang, Y.X., Ma, T.T. and Ge, Y.J. (2015), "Evaluation on bridge dynamic properties and VIV performance based on wind tunnel test and field measurement", *Wind. Struct.*, **20**(6), 719-737.

JH